Kinematic Analysis and Dynamic Control of a 3-PUU Parallel Manipulator for Cardiopulmonary Resuscitation

Yangmin Li and Qingsong Xu
Dept. of Electromechanical Engineering, Faculty of Science and Technology, University of Macau
Av. Padre Tomás Pereira S.J., Taipa, Macao SAR, P. R. China
Email: ymli@umac.mo, ya47401@umac.mo

Abstract— **The concept of a medical parallel manipulator applicable to chest compression in the process of cardiopulmonary resuscitation (CPR) is proposed in this paper. According to the requirement of CPR action, a three-prismatic-universal-universal (3-PUU) translational parallel manipulator (TPM) is designed for such applications. And a thorough analysis involving the issues of kinematics, dynamics, and control have been performed for the 3-PUU TPM. Not only the inverse and forward kinematics problems are solved in closed-form, but also the Jacobian matrix is derived analytically, along with the manipulator workspace generated in view of the physical constraints imposed by mechanical joints. Based on the principle of virtual work with a simplifying hypothesis adopted, the dynamic modeling is performed, and dynamic control utilizing computed torque method is implemented, at last the simulation results illustrate the well performance of the control algorithm. The research work provide a sound base for the development of a medical manipulator to assist in CPR operation.**

I. Introduction

Cardiopulmonary resuscitation (CPR) is a combination of rescue breathing (mouth-to-mouth resuscitation) and chest compressions delivered to victims thought to be in cardiac arrest, and the goal of CPR is to maintain oxygenated blood flow to vital organs and to prevent anoxic tissue damage during cardiac arrest [1]. If a person is not breathing or circulating blood adequately, CPR can restore circulation of oxygen-rich blood to the brain. Without oxygen, permanent brain damage or death can occur in less than 10 minutes. For a large number of patients who undergo unexpected cardiac arrest, the only hope of survival is timely and appropriate CPR.

The compression for adult CPR is at the rate of about 100 times per minute with the depth of 4 to 5 centimeters using two hands, and the CPR is usually performed by two rescuers with the compression-to-ventilation ratio of 15 compressions to 2 breaths [2]. But when there is only one rescuer or the rescuer is unable to perform chest compressions, a medical robot applicable to chest compressions is highly required. In this paper, we propose the concept design of a medical parallel manipulator to assist in CPR.

Parallel mechanical architectures were first introduced in tire testing by Gough, and later were used by Stewart as motion simulators. A parallel manipulator typically consists of a moving platform that is connected to a fixed base by several limbs or legs in parallel. Nowadays, parallel manipulators are applied widely since they possess many inherent advantages such as high speed, high accuracy, high stiffness, and high load carrying capacity over their serial counterparts. An exhaustive enumeration of parallel robots' mechanical architectures and their versatile applications can be found in [3].

Fig. 1. A schematic of CPR operation.

In particular, parallel manipulators have great potential applications in medical field due to their well performance in high structural stiffness and motion accuracy, and compact structures, etc. For instance, using a parallel robot, a compact surgical robot system was developed for image-guided orthopedic surgery in [4], a new approach to robot-assisted spine and trauma surgery was presented in [5] utilizing a designed six-degree-of-freedom (6-DOF) parallel manipulator, the mouth opening and closing training for the rehabilitation of patients who have problems on the jaw joint was suggested in [6] with a 6-DOF parallel robot, a 4-DOF parallel wire-driven mechanism was presented in [7] with applications to leg rehabilitation, and reference [8] proposed an idea of applying parallel robots to surgical treatments with monitoring real time images, etc. However, there are few literatures dealing with parallel manipulators applying in CPR assistant.

The remainder of this paper is organized in the following way: The concept design of the medical manipulator and its architecture selection are presented in Section II. The kinematic models and Jacobian matrix are derived in Section III. Considering the physical constraints introduced by mechanical joints, the reachable workspace of the medical manipulator is generated in Section IV. Then the dynamic modeling of the manipulator is carried out in Section V, and dynamic control method is implemented in Section VI with computer simulations illustrated. Finally, some concluding remarks are given in Section VII.

0-7803-9177-2/05/$20.00/©2005 IEEE

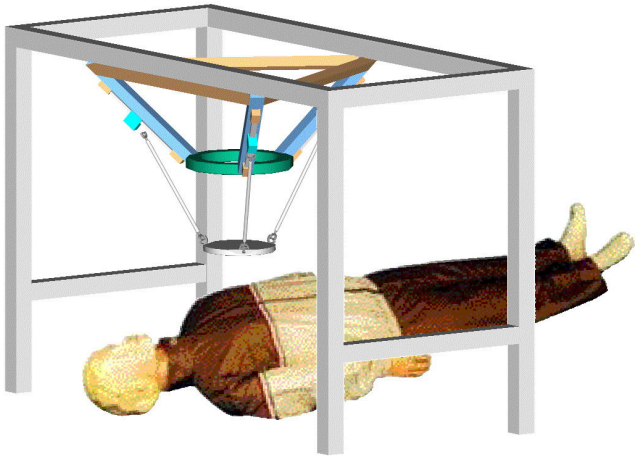

Fig. 2. A 3-PUU medical parallel manipulator.

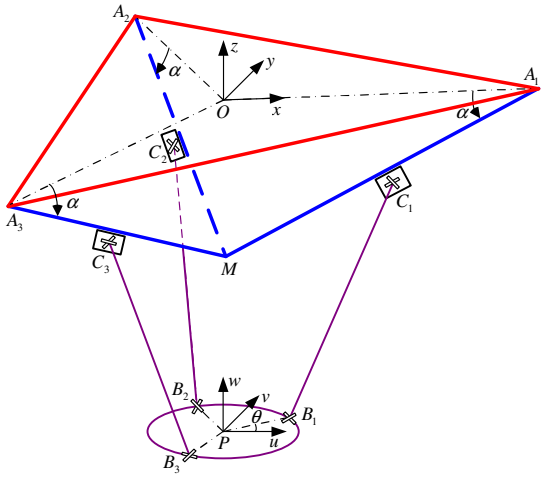

Fig. 3. Schematic representation of a 3-PUU TPM.

II. Concept Design of a Medical Parallel Manipulator

A. Concept Design

A schematic of CPR performing is shown in Fig. 1, and a CAD model of the designed medical robot is illustrated in Fig. 2. Due to some merits mentioned above, parallel mechanisms are employed to design a manipulator applicable to chest compressions in CPR. In fact, this is the main reason why the rescuer uses two hands instead of only one hand to perform the action of chest compressions. When performing chest compressions, the two arms of the rescuer construct a parallel mechanism indeed. In addition, we utilize a 3-PUU parallel mechanism with fixed actuators to build such a robot. It is demonstrated that a 3-PUU mechanism can be arranged to achieve only translational motions with some certain geometric conditions satisfied [9]–[11], i.e., in each kinematic chain, the first revolute joint axis is parallel to the last revolute joint axis, and the two intermediate joint axes are parallel to each other.

The reason of utilizing a 3-PUU translational parallel manipulator (TPM) with fixed actuators lies in that in chest compressions process, the mainly used motion of the manipulator is the vertical translation. In addition to a translation in the z axis direction, a 3-PUU TPM can also provide the translations in the x and y axis direction, which enables the adjusting of the manipulator moving platform to a suitable position for chest compression performing. Moreover, the fixed actuators make it possible that the moving components of the manipulator do not bear the load of the actuators. This enables large powerful actuators to drive relatively small structures, facilitating the design of the manipulator with faster, stiffer, and stronger characteristics.

According to the criterions to design such a medical robot, other kinds of parallel manipulators can also be employed into the application fields of CPR assistance.

B. Architecture Design

To design a 3-PUU medical manipulator, there are many factors to take into account. It is now well known that parallel manipulators possess relatively limited workspace compared with their serial counterparts. Thus it is natural to design a parallel manipulator with a workspace as large as possible to enhance its working capability [12]. At the same time, in order to generate an architecture as compact as possible, it is necessary to design a medical manipulator utilizing an index of space utility ratio, which is proposed to penalize designs possessing large physical size yet producing relatively small workspace [13]. Additionally, high dexterity performance is also required to design a parallel manipulator such that it can perform dexterous operation within its workspace [14].

In this work, we design the architectural parameters of a 3-PUU medical TPM applicable to CPR action utilizing the optimization methodology presented in [13] by making a comprise between the performance of global dexterity index over the entire workspace and space utility ratio index which is defined as the ratio of total workspace volume to physical size of the robot. Let the stroke of linear actuators be $\Delta d = 100\,\text{mm}$. The optimized architectural parameters of the 3-PUU TPM is described in the following Table I.

III. Kinematic Analysis

A. Architecture Description

Fig. 3 represents the schematic diagram of a 3-PUU TPM, which consists of a moving platform, a fixed base, and three limbs with identical kinematic structure. Each limb connects the fixed base to the moving platform by a prismatic (P) joint followed by two universal (U) joints in sequence, where the P joint is driven by a linear actuator.

Since each U joint consists of two intersecting revolute joints, each limb is kinematically equivalent to a PRRRR chain. Because the geometric conditions stated in Section II do not require the U joint axes to intersect at a point, any 3-PRRRR structure parallel manipulators whose revolute joint

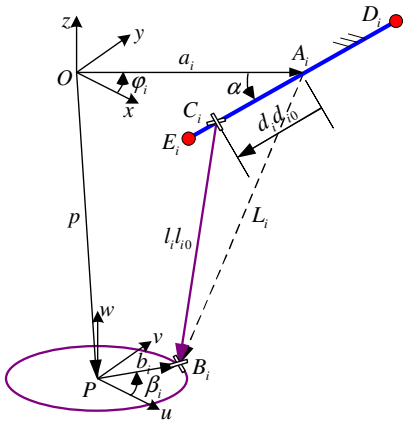

Fig. 4. Geometry of one typical kinematic chain.

axes satisfy the aforementioned conditions will achieve a pure translational motion.

For the purpose of analysis, as represented in Fig. 3 and 4, we assign a fixed Cartesian coordinate system $O\{x, y, z\}$ at the centered point O of the fixed base platform $\Delta A_1A_2A_3$, and a moving Cartesian frame $P\{u, v, w\}$ on the moving platform at the centered point P of triangle $\Delta B_1B_2B_3$. For simplification and without the loss of generality, let the x axis and u axis be parallel to one another, and the x axis direct along $\overrightarrow{OA_1}$. Vector $\overrightarrow{OA_i}$ ($i = 1, 2, 3$) is not necessarily parallel to vector $\overrightarrow{PB_i}$, and the angle between them is defined as the twist angle θ, i.e., the angle between the moving platform and the fixed base. The three rails D_iE_i intersect one another at point M, and intersect the x-y plane at points A_1, A_2, and A_3, that lie on a circle of radius a. The three links C_iB_i with the lengths of l intersect the u-v plane at points B_1, B_2, and B_3, which lie on a circle of radius b. The sliders of the P joints are restricted to move along the rails between D_i and E_i. Angle α is measured from the fixed base to rails D_iE_i and is defined as the actuators layout angle. Angle φ_i is measured from the x axis to $\overrightarrow{OA_i}$ in the fixed frame, and angle β_i is from the u axis to $\overrightarrow{PB_i}$ in the moving frame. In order to generate a symmetric workspace of the manipulator, we assign that $\varphi_i = (i-1) \times 120\,^\circ$ and $\beta_i = \theta + (i-1) \times 120\,^\circ$, for $i = 1$, 2, and 3.

B. Kinematic Modeling

As shown in Fig. 4, the position vectors of points A_i and B_i with respect to frames O and P respectively can be written as

$$^O\mathbf{a}_i = [ac\varphi_i \quad as\varphi_i \quad 0]^T, \tag{1}$$

$$^P\mathbf{b}_i = [bc\beta_i \quad bs\beta_i \quad 0]^T, \tag{2}$$

where c stands for cosine, s stands for sine, and a leading superscript indicates the coordinate frame at which a vector is located. For brevity, the leading superscript will be omitted whenever the coordinate frame is the fixed base frame, e.g., $^O\mathbf{a}_i = \mathbf{a}_i$.

Generally, the position and orientation of the moving platform with respect to the fixed frame can be described by a position vector, $\mathbf{p} = \overrightarrow{OP} = [p_x \quad p_y \quad p_z]^T$, and a 3×3 rotation matrix $^O\mathbf{R}_P$. However, since the moving platform possesses only a translational motion, $^O\mathbf{R}_P$ becomes an identity matrix. Then, we have $^P\mathbf{b}_i = \mathbf{b}_i$.

TABLE I
ARCHITECTURAL PARAMETERS OF THE DESIGNED 3-PUU TPM

Parameter	Value	Unit
a	150.0	mm
b	50.0	mm
l	150.0	mm
α	45.0	°
θ	0.0	°

1) Inverse Kinematic Modeling: The inverse kinematics problem solves the actuated variables from a given position of the moving platform.

Referring to Fig. 4, a vector-loop equation can be written for the ith limb as

$$l\,\mathbf{l}_{i0} = \mathbf{L}_i - d_i\mathbf{d}_{i0}\,, \tag{3}$$

with

$$\mathbf{L}_i = \mathbf{p} + \mathbf{b}_i - \mathbf{a}_i\,, \tag{4}$$

where $\mathbf{l}_{i0}$ is the unit vector along C_iB_i, d_i represents the linear displacement of the ith actuator, and $\mathbf{d}_{i0}$ is the corresponding unit vector pointing along rail D_iE_i, which can be expressed as

$$\mathbf{d}_{i0} = [-c\alpha c\varphi_i \quad -c\alpha s\varphi_i \quad -s\alpha]^T\,. \tag{5}$$

Dot-multiplying (3) with itself and rearranging the terms, yields

$$d_i^2 - 2d_i\mathbf{d}_{i0}^T\mathbf{L}_i + \mathbf{L}_i^T\mathbf{L}_i - l^2 = 0\,. \tag{6}$$

Solving (6) allows the generation of the inverse kinematic solutions:

$$d_i = \mathbf{d}_{i0}^T\mathbf{L}_i \pm \sqrt{(\mathbf{d}_{i0}^T\mathbf{L}_i)^2 - \mathbf{L}_i^T\mathbf{L}_i + l^2}\,. \tag{7}$$

We can see that there exist two solutions for each actuator. To enhance the stiffness of the medical manipulator, only the negative square roots in (7) are selected to yield a unique solution where the three legs are inclined inward from top to bottom.

2) Forward Kinematic Modeling: Given a set of the actuated inputs, the positions of the moving platform are solved by the forward kinematics.

Combining (3) with (4), we can get

$$l\,\mathbf{l}_{i0} = \mathbf{p} - \mathbf{e}_i\,, \tag{8}$$

with $\mathbf{e}_i = \mathbf{a}_i + d_i\mathbf{d}_{i0} - \mathbf{b}_i$.

Dot-multiplying (8) with itself and rearranging the items, yields

$$\mathbf{p}^T\mathbf{p} - 2\mathbf{p}^T\mathbf{e}_i + \mathbf{e}_i^T\mathbf{e}_i = l^2\,. \tag{9}$$

Writing (9) three times, once for each $i = 1$, 2, and 3, leads to three equations in $\mathbf{p}$. Each equation represents a sphere of radius l with the center located at the end point N_i of a vector

defined by point O and $\mathbf{e}_i$. The intersection of these spheres yields the solutions to the forward kinematics.

Subtracting (9) for $i = 1$ from (9) for $i = 2$ and 3, respectively, yields

$$\mathbf{p}^T(\mathbf{e}_2 - \mathbf{e}_1) - h_2 = 0\,, \tag{10}$$
$$\mathbf{p}^T(\mathbf{e}_3 - \mathbf{e}_1) - h_3 = 0\,, \tag{11}$$

where $h_2 = (\mathbf{e}_2^T\mathbf{e}_2 - \mathbf{e}_1^T\mathbf{e}_1)/2$, $h_3 = (\mathbf{e}_3^T\mathbf{e}_3 - \mathbf{e}_1^T\mathbf{e}_1)/2$. Equations (10) and (11) represent two linear functions in three unknowns of p_x, p_y, and p_z, from which p_x and p_y can be expressed in terms of p_z as:

$$p_x = k_1 + p_z k_2\,, \tag{12}$$
$$p_y = k_3 + p_z k_4\,, \tag{13}$$

where $k_1 = S_1/S_{01}$, $k_2 = S_2/S_{01}$, $k_3 = S_3/S_{02}$, $k_4 = S_4/S_{02}$, with $S_1 = h_2(e_{3y} - e_{1y}) - h_3(e_{2y} - e_{1y})$, $S_2 = (e_{3z} - e_{1z})(e_{2y} - e_{1y}) - (e_{2z} - e_{1z})(e_{3y} - e_{1y})$, $S_{01} = (e_{2x} - e_{1x})(e_{3y} - e_{1y}) - (e_{3x} - e_{1x})(e_{2y} - e_{1y})$, $S_3 = h_2(e_{3x} - e_{1x}) - h_3(e_{2x} - e_{1x})$, $S_4 = (e_{3z} - e_{1z})(e_{2x} - e_{1x}) - (e_{2z} - e_{1z})(e_{3x} - e_{1x})$, $S_{02} = (e_{2y} - e_{1y})(e_{3x} - e_{1x}) - (e_{3y} - e_{1y})(e_{2x} - e_{1x})$, and e_{ix}, e_{iy}, and e_{iz} denote the x, y, and z components of vector $\mathbf{e}_i$, respectively.

Substituting (12) and (13) into (9) for $i = 1$, yields

$$T_1 p_z^2 + 2T_2 p_z + T_3 = 0\,, \tag{14}$$

where $T_1 = k_2^2 + k_4^2 + 1$, $T_2 = k_1k_2 + k_3k_4 - e_{1x}k_2 - e_{1y}k_4 - e_{1z}$, $T_3 = k_1^2 + k_3^2 - 2e_{1x}k_1 - 2e_{1y}k_3 - l^2$.

Solving (14), results in

$$p_z = \frac{-T_2 \pm \sqrt{T_2^2 - T_1T_3}}{T_1}\,. \tag{15}$$

Thus, (12), (13), and (15) represent the forward kinematic solutions.

When there are two different real solutions, the two corresponding points form a mirror image of each other about the plane defined by the three sphere center points N_1, N_2, and N_3. Thus, one point is located below the actuators, and the other one above. Only the point below the actuators is taken into consideration for real applications, since the point above the actuators could only be obtained by reassembling the manipulator. And the unique feasible configuration is an important feature for real time control in robotic applications.

C. Jacobian Matrix Generation

Substituting (4) into (3) and differentiating it with respect to time, yields

$$\dot{d}_i\mathbf{d}_{i0} = \dot{\mathbf{x}} - l\,\boldsymbol{\omega}_i \times \mathbf{l}_{i0}\,, \tag{16}$$

where $\boldsymbol{\omega}_i$ denotes the vectors of angular velocities for link C_iB_i with respect to the fixed frame, and $\dot{\mathbf{x}} = [\dot{p}_x \quad \dot{p}_y \quad \dot{p}_z]^T$ is the vector of linear velocities for the moving platform.

Dot-multiplying both sides of (16) by $\mathbf{l}_{i0}$, yields

$$\mathbf{l}_{i0}^T\mathbf{d}_{i0}\dot{d}_i = \mathbf{l}_{i0}^T\dot{\mathbf{x}}\,. \tag{17}$$

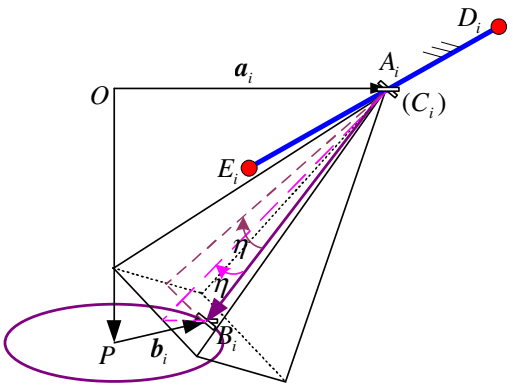

Fig. 5. Cone angle limits of a universal joint.

Writing (17) three times, once for $i = 1$, 2, and 3, yields three scalar equations, which can be written in matrix form as

$$\mathbf{J}_q\dot{\mathbf{q}} = \mathbf{J}_x\dot{\mathbf{x}}\,, \tag{18}$$

where

$$\mathbf{J}_q = \begin{bmatrix} \mathbf{l}_{10}^T\mathbf{d}_{10} & 0 & 0 \\ 0 & \mathbf{l}_{20}^T\mathbf{d}_{20} & 0 \\ 0 & 0 & \mathbf{l}_{30}^T\mathbf{d}_{30} \end{bmatrix},\ \mathbf{J}_x = \begin{bmatrix} \mathbf{l}_{10}^T \\ \mathbf{l}_{20}^T \\ \mathbf{l}_{30}^T \end{bmatrix},$$

and $\dot{\mathbf{q}} = [\dot{d}_1 \quad \dot{d}_2 \quad \dot{d}_3]^T$ is the vector of actuated joint rates.

When the manipulator is away from singularities, from (18), we can obtain

$$\dot{\mathbf{q}} = \mathbf{J}\,\dot{\mathbf{x}}\,, \tag{19}$$

where

$$\mathbf{J} = \mathbf{J}_q^{-1}\mathbf{J}_x \tag{20}$$

is the 3×3 Jacobian matrix of a 3-PUU TPM, which relates the output velocities to the actuated joint rates.

IV. Workspace Determination

The reachable workspace of a 3-PUU TPM can be defined as the space that can be reached by the reference point P.

A. Physical Constraints

In the design of a 3-PUU TPM, some physical constraints should be taken into considerations, such as the limits of cone angles of the U joints and motioning ranges of the linear actuators. Here, we mainly discuss the constraints introduced by cone angle limits of the U joints.

The two cone angle limits (η) of one U joint are represented in Fig. 5. For the ith PUU kinematic chain at the home position, as illustrated in Fig. 6(a), the two outer revolute joint axes which are parallel to each other are arranged to be perpendicular to the direction of link C_iB_i and lie in plane 1 which is parallel to the z axis, and the two inner revolute joint axes which are parallel to each other are arranged to be perpendicular to vector $\overrightarrow{C_iB_i}$ and lie in plane 2 which is perpendicular to plane 1.

For the universal joint C_i, the cone angle of the outer revolute joint is defined as the angle γ_{i1} between link C_iB_i and

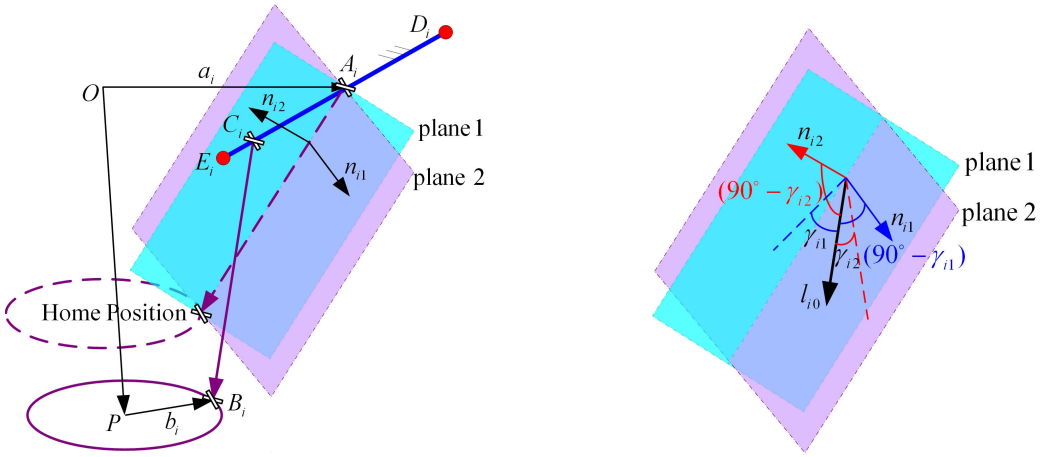

(a) Normal vectors of plane 1 and plane 2.

(b) Cone angles representation.

Fig. 6. Solve the cone angles of an universal joint.

plane 1, and cone angle of the inner revolute joint is defined as the angle γ_{i2} between link C_iB_i and plane 2, as described in Fig. 6(b), respectively. Considering the relationship between normal vectors of the planes and direction vector of the link, the two cone angles can be solved as follows.

$$\gamma_{i1} = \sin^{-1}\left(\frac{\mathbf{n}_{i1}^T\mathbf{l}_{i0}}{\|\mathbf{n}_{i1}\|}\right), \tag{21}$$

$$\gamma_{i2} = \sin^{-1}\left(\frac{\mathbf{n}_{i2}^T\mathbf{l}_{i0}}{\|\mathbf{n}_{i2}\|}\right), \tag{22}$$

where $\mathbf{n}_{i1}$ and $\mathbf{n}_{i2}$ denote the normal vectors of plane 1 and plane 2, respectively.

We assume that the cone angle limits of the U joints are $\eta = 20°$, and motioning range limits of the P joints are $\pm\Delta d/2$, i.e., $-20^\circ \le \gamma_{i1}, \gamma_{i2} \le 20^\circ$ and $-50\,\text{mm} \le d_i \le 50\,\text{mm}$, for $i = 1$, 2, and 3.

B. Algorithms

Utilizing the approach of changing the coordinates of three P joints within their motioning ranges and resorting to the forward kinematic solutions, the workspace shape can be easily expressed in 3-D space by a series of dots. From the derived results, it is observed that there exists no any void within the workspace, i.e., the cross section of workspace is consecutive at every height. This allows us to slice the whole workspace of the manipulator into a series of sub-workspaces that are parallel to the base platform, then adopt a numerical search method to determine the boundary of each sub-workspace, and calculate the volume of the reachable workspace quantitatively [15]. This process is based on the inverse kinematic solutions and with the consideration of the physical constraints mentioned above.

The following Fig. 7 shows the workspace of a 3-PUU TPM with the architectural parameters described in Table I. It is seen that the reachable workspace is 120 degree-symmetrical about the three actuators' motioning directions when looked down. In the upper and lower range of the workspace, the cross section has the triangular shape, while in the dominate middle range of the workspace, the cross sectional shape looks like a hexagon. And the workspace range in the z axis direction is 141.4 mm, which is enough for the application in CPR performing.

V. Dynamic Modeling

The main issue in dynamic analysis for a parallel manipulator is to develop an inverse dynamic model, which enables the computation of the required actuator forces and/or torques when given a desired trajectory of the moving platform. In following section, we will perform the dynamic modeling of the 3-PUU TPM via the virtual work principle.

A. Dynamics Analysis

1) Simplification Hypothesis: As for a 3-PUU TPM, similar to a 3-PRS parallel manipulator [16], the complexity of the dynamic model partly comes from the three moving legs. Since the legs can be built with light materials such as the aluminium alloy, we can simplify the dynamic problem by the following hypotheses:

1) the rotational inertias of legs are neglected;
2) the mass of each leg is equally divided into two portions and placed at its two extremities, i.e., one half at its upper extremity (slider) and the other half at its lower extremity (moving platform).

Let m_p, m_s, and m_l denote the mass of the moving platform, one slider, and one leg, respectively. Then, the equivalent mass of the slider and the moving platform respectively becomes

$$\hat{m}_s = m_s + \frac{1}{2}m_l\,, \quad \hat{m}_p = m_p + \frac{3}{2}m_l\,.$$

2) Dynamic Modeling: Let $\boldsymbol{\tau} = [f_1 \quad f_2 \quad f_3]^T$ be the vector of actuator forces, and $\delta\mathbf{q} = [\delta d_1 \quad \delta d_2 \quad \delta d_3]^T$ be the vector of corresponding virtual displacements. Additionally, let $\delta\mathbf{x} = [\delta p_x \quad \delta p_y \quad \delta p_z]^T$ represent the vector of virtual linear displacements of the moving platform. Applying the principle

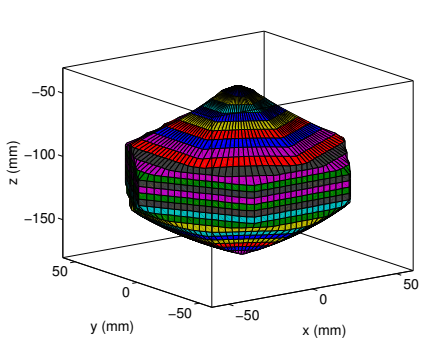

(a) Three-dimensional view.

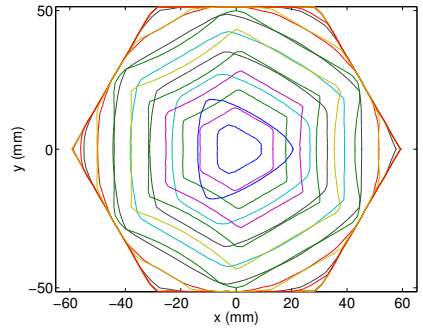

(b) Top view.

Fig. 7. Reachable workspace of a 3-PUU TPM.

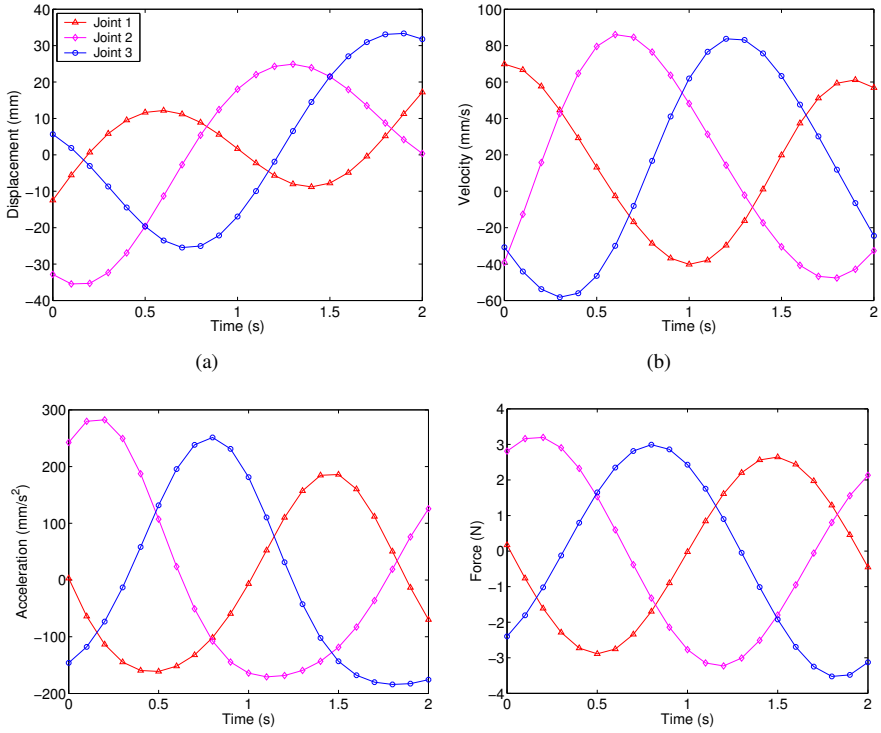

(a) (b) (c) (d)

Fig. 8. Simulation results for time history of joint (a) displacements, (b) velocities, (c) accelerations, and (d) forces.

of virtual work, allows the derivation of the following equation by neglecting the friction forces in joints and assuming that there is no external force suffered.

$$\boldsymbol{\tau}^T\delta\mathbf{q} + \mathbf{G}_s^T\delta\mathbf{q} - \mathbf{F}_s^T\delta\mathbf{q} + \mathbf{G}_p^T\delta\mathbf{x} - \mathbf{F}_p^T\delta\mathbf{x} = 0\,, \tag{23}$$

where $\mathbf{G}_s = [\hat{m}_s g s\alpha \quad \hat{m}_s g s\alpha \quad \hat{m}_s g s\alpha]^T$ is the vector of gravity forces of the sliders with g represents the gravity acceleration, $\mathbf{G}_p = [0 \quad 0 \quad \hat{m}_p g]^T$ is the gravity force vector of the moving platform, $\mathbf{F}_s = [\hat{m}_s\ddot{d}_1 \quad \hat{m}_s\ddot{d}_2 \quad \hat{m}_s\ddot{d}_3]^T$ denotes the vector of inertial forces of the sliders, and $\mathbf{F}_p = [\hat{m}_p\ddot{p}_x \quad \hat{m}_p\ddot{p}_y \quad \hat{m}_p\ddot{p}_z]^T$ represents the vector of inertial forces of the moving platform.

From (19), we can obtain

$$\dot{\mathbf{x}} = \mathbf{J}^{-1}\dot{\mathbf{q}}\,, \tag{24}$$

consequently

$$\delta\mathbf{x} = \mathbf{J}^{-1}\,\delta\mathbf{q}\,. \tag{25}$$

Substituting (25) into (23), yields

$$(\boldsymbol{\tau}^T + \mathbf{G}_s^T - \mathbf{F}_s^T + \mathbf{G}_p^T\mathbf{J}^{-1} - \mathbf{F}_p^T\mathbf{J}^{-1})\delta\mathbf{q} = 0\,. \tag{26}$$

Since (26) holds for any virtual displacements $\delta\mathbf{q}$, we have

$$\boldsymbol{\tau} = \mathbf{F}_s + \mathbf{J}^{-T}\mathbf{F}_p - \mathbf{G}_s - \mathbf{J}^{-T}\mathbf{G}_p\,. \tag{27}$$

Substituting the inertial forces into (27), yields

$$\boldsymbol{\tau} = \mathbf{M}_s\ddot{\mathbf{q}} + \mathbf{J}^{-T}\mathbf{M}_p\ddot{\mathbf{x}} - \mathbf{G}_s - \mathbf{J}^{-T}\mathbf{G}_p\,, \tag{28}$$

where $\mathbf{M}_s = \hat{m}_s\,\mathrm{diag}\{1\ 1\ 1\}$, $\mathbf{M}_p = \hat{m}_p\,\mathrm{diag}\{1\ 1\ 1\}$, i.e.,

$$\mathbf{M}_s = \begin{bmatrix} \hat{m}_s & 0 & 0 \\ 0 & \hat{m}_s & 0 \\ 0 & 0 & \hat{m}_s \end{bmatrix}, \quad \mathbf{M}_p = \begin{bmatrix} \hat{m}_p & 0 & 0 \\ 0 & \hat{m}_p & 0 \\ 0 & 0 & \hat{m}_p \end{bmatrix}.$$

Differentiating (24) with respect to time, yields

$$\ddot{\mathbf{x}} = \mathbf{J}^{-1}\ddot{\mathbf{q}} + \dot{\mathbf{J}}^{-1}\dot{\mathbf{q}}\,. \tag{29}$$

Substituting (29) into (28), yields

$$\boldsymbol{\tau} = \mathbf{M}(\mathbf{q})\ddot{\mathbf{q}} + \mathbf{C}(\mathbf{q},\dot{\mathbf{q}})\dot{\mathbf{q}} + \mathbf{G}(\mathbf{q})\,, \tag{30}$$

where

$$\begin{aligned} \mathbf{M}(\mathbf{q}) &= \mathbf{M}_s + \mathbf{J}^{-T}\mathbf{M}_p\mathbf{J}^{-1}\,, \\ \mathbf{C}(\mathbf{q},\dot{\mathbf{q}}) &= \mathbf{J}^{-T}\mathbf{M}_p\dot{\mathbf{J}}^{-1}\,, \\ \mathbf{G}(\mathbf{q}) &= -\mathbf{G}_s - \mathbf{J}^{-T}\mathbf{G}_p\,, \end{aligned}$$

and $\mathbf{q} \in \mathbb{R}^3$ denotes the controlled variables, $\mathbf{M}(\mathbf{q}) \in \mathbb{R}^{3\times3}$ is a symmetric positive definite inertial matrix, $\mathbf{C}(\mathbf{q},\dot{\mathbf{q}}) \in \mathbb{R}^{3\times3}$ represents the matrix of centrifugal and Coriolis forces, and $\mathbf{G}(\mathbf{q}) \in \mathbb{R}^3$ is the vector of gravity forces.

Equation (30) represents the joint space dynamic model of a 3-PUU TPM.

B. Simulations

Although the most important motion of the medical manipulator to assist in CPR is the back and forth translations in

TABLE II
DYNAMIC PARAMETERS OF THE PARALLEL MANIPULATOR

Parameter	Value	Unit
m_p	0.4	kg
m_s	0.4	kg
m_l	0.2	kg
g	9.8	m/s^2

vertical direction, a complex trajectory of the moving platform described as follows is considered for the simulation study in order to demonstrate the dynamic model.

$$\begin{aligned} p_x &= -30\sin(\pi t)\,, \\ p_y &= 30\cos(\pi t)\,, \\ p_z &= -110 + 20\cos(\frac{\pi}{2}t)\,, \end{aligned} \tag{31}$$

where t is the time variable, and p_x, p_y, and p_z are in unit of millimeters.

The architectural and dynamic parameters of the 3-PUU TPM are represented in Table I and II, respectively. And the simulation results are shown in Fig. 8, where (a) to (c) describe the time history of joint displacements, velocities, and accelerations, respectively, which are derived via the inverse kinematic solutions. And Fig. 8(d) illustrates the time history of joint forces generated from the dynamic model.

VI. DYNAMIC CONTROL

In this section, we implement the dynamic control in joint space utilizing the computed torque method for a 3-PUU TPM.

A. Control Algorithm

Joint space dynamic model (30) can be rewritten in the following form:

$$\boldsymbol{\tau} = \mathbf{M}(\mathbf{q})\ddot{\mathbf{q}} + \mathbf{H}(\mathbf{q}, \dot{\mathbf{q}})\,, \tag{32}$$

with $\mathbf{H}(\mathbf{q}, \dot{\mathbf{q}}) = \mathbf{C}(\mathbf{q}, \dot{\mathbf{q}})\dot{\mathbf{q}} + \mathbf{G}(\dot{\mathbf{q}})$.

Fig. 9 shows a block diagram of the computed torque control system with proportional-derivative (PD) feedback. Assuming that there are no external disturbances, then the manipulator is actuated with the following vector of joint forces.

$$\boldsymbol{\tau} = \hat{\mathbf{M}}(\mathbf{q})\mathbf{u} + \hat{\mathbf{H}}(\mathbf{q}, \dot{\mathbf{q}})\,, \tag{33}$$

where $\mathbf{u}$ is an input signal vector in the form of acceleration, $\hat{\mathbf{M}}(\mathbf{q})$ and $\hat{\mathbf{H}}(\mathbf{q}, \dot{\mathbf{q}})$ denote the estimators of the inertial matrix $\mathbf{M}(\mathbf{q})$ and the nonlinear coupling matrix $\mathbf{H}(\mathbf{q}, \dot{\mathbf{q}})$ implemented in the controller, respectively.

Combining (32) and (33), results in the following linear second order system

$$\ddot{\mathbf{q}} = \mathbf{u}\,. \tag{34}$$

The obtained linear system allows the specification of the necessary feedback gains as well as the reference signal required for a desired motion task. Depending on the desired closed-loop system response, there are many possible choices for the reference signal. For perfect tracking in a PD feedback

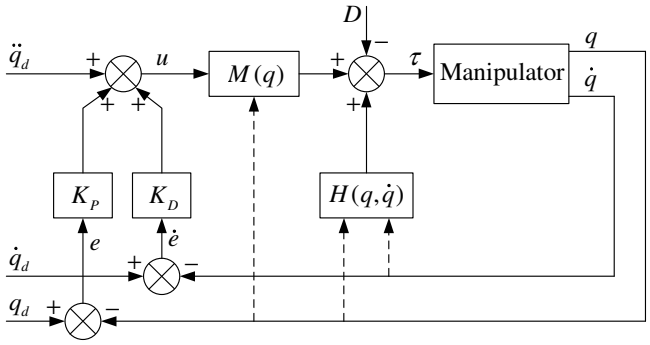

Fig. 9. Block diagram of joint space dynamic control for a 3-PUU TPM.

implementation, the reference signal is defined according to the following algorithms [17]:

$$\mathbf{r} = \ddot{\mathbf{q}}_d + \mathbf{K}_D\dot{\mathbf{q}}_d + \mathbf{K}_P\mathbf{q}_d\,, \tag{35}$$

where $\mathbf{q}_d$ denotes the desired joint trajectory, $\mathbf{K}_P$ and $\mathbf{K}_D$ denote the symmetric positive definite feedback gains matrices.

The acceleration input signal in (34) then becomes

$$\begin{aligned} \mathbf{u} &= \mathbf{r} - \mathbf{K}_D\dot{\mathbf{q}} - \mathbf{K}_P\mathbf{q} \\ &= \ddot{\mathbf{q}}_d + \mathbf{K}_D(\dot{\mathbf{q}}_d - \dot{\mathbf{q}}) + \mathbf{K}_P(\mathbf{q}_d - \mathbf{q})\,. \end{aligned} \tag{36}$$

Substituting (36) into (34), leads to the equation of errors as follows:

$$\ddot{\mathbf{e}} + \mathbf{K}_D\dot{\mathbf{e}}_d + \mathbf{K}_P\mathbf{e} = 0\,, \tag{37}$$

where $\mathbf{e} = \mathbf{q}_d - \mathbf{q}$ is the vector of joint tracking errors.

The tracking error will go to zero asymptotically by specifying appropriate values of feedback gains $\mathbf{K}_P$ and $\mathbf{K}_D$. It is shown that the computed torque control method is robust to small modeling errors [18].

B. Simulation Results

The dynamic control algorithm is implemented such that the P joint can track a trajectory as described in Fig. 8(a), and the simulations are performed with Matlab and Simulink softwares. In the simulation, the feedback gains are set to $\mathbf{K}_P = 625\,\mathrm{diag}\{1\ 1\ 1\}$, and $\mathbf{K}_D = 50\,\mathrm{diag}\{1\ 1\ 1\}$.

The simulation results are shown in Fig. 10, where figures (a), (b), and (c) represent the actuated joint displacement errors, the moving platform position errors, and the actuated joint forces, respectively. It is observed that both the joint space errors and task space errors converge to zero after about 0.3 seconds. The simulation results illustrate that the 3-PUU TPM can be controlled by this method, and also show that the introduced simplifying hypothesis is reasonable.

VII. CONCLUSION

In this paper, we have introduced the concept of a medical parallel manipulator applicable to chest compression in the process of CPR.

To meet the needs of reducing the workload of doctors in performing CPR, a 3-PUU TPM is designed. The kinematic analysis has been performed with both the inverse and

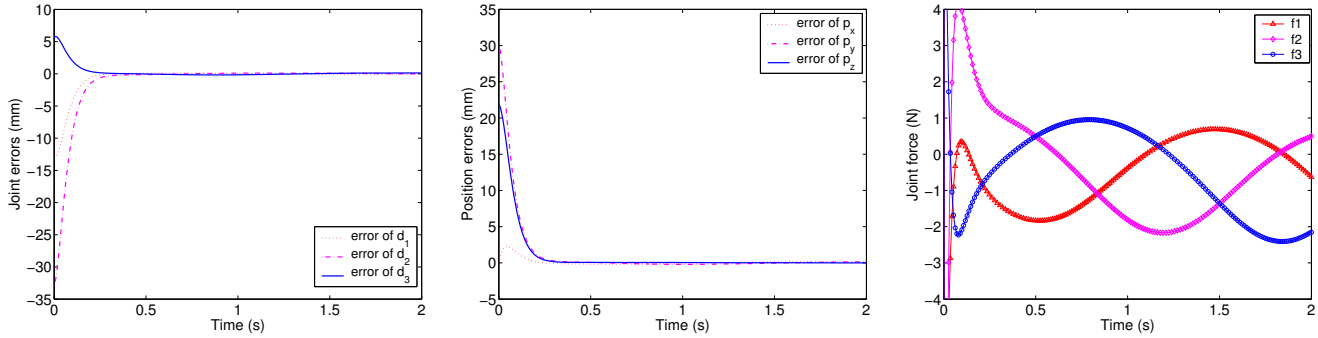

(a) Joint tracking errors. (b) Position errors. (c) Joint forces.

Fig. 10. Simulation results of dynamic control method.

forward kinematic solutions derived in closed-form and the Jacobian matrix generated analytically. Taking into account the physical constraints introduced by the cone angle limits of universal joints and motioning range limits of prismatic joints, the manipulator reachable workspace is determined via a numerical search method. By employing a simplification hypothesis and resorting to the approach of virtual work principle, the inverse dynamic model is established, which is illustrated by simulations. Based upon the derived dynamic model, the dynamic control in joint space utilizing computed torque method has been implemented, and simulation results illustrate the rationality of the adopted simplifying hypothesis and the well performance of the control algorithm.

The studies presented here provide a sound base to develop a medical manipulator to assist in CPR operation. Further work will focus on building up the manipulator prototype and establishing system models involving the interaction between the mobile platform and the human body through applying force control or hybrid force/position control methods.

ACKNOWLEDGMENT

The authors appreciate the fund support from the research committee of University of Macau under grant no.: RG083/04-05S/LYM/FST.

REFERENCES

[1] I. N. Bankman, K. G. Gruben, H. R. Halperin, A. S. Popel, A. D. Guerci, and J. E. Tsitlik, "Identification of dynamic mechanical parameters of the human chest during manual cardiopulmonary resuscitation," *IEEE Trans. Biomed. Eng.*, vol. 37, no. 2, pp. 211–217, 1990.

[2] http://www.health.harvard.edu/fhg/firstaid/CPRadult.shtml, 2003.

[3] J.-P. Merlet, *Parallel Robots*. London: Kluwer Academic Publishers, 2000.

[4] G. Brandt, A. Zimolong, L. Carrat, P. Merloz, H.-W. Staudte, S. Lavallée, K. Radermacher, and G. Rau, "CRIGOS: A compact robot for image-guided orthopedic surgery," *IEEE Trans. Inform. Technol. Biomed.*, vol. 3, no. 4, pp. 252–260, 1999.

[5] M. Shoham, E. Zehavi, L. Joskowicz, E. Batkilin, and Y. Kunicher, "Bone-mounted miniature robot for surgical procedures: Concept and clinical applications," *IEEE Trans. Robot. Automat.*, vol. 19, no. 5, pp. 893–901, 2003.

[6] H. Takanobu, T. Maruyama, A. Takanishi, K. Ohtsuki, and M. Ohnishi, "Mouth opening and closing training with 6-DOF parallel robot," in *Proc. of IEEE Int. Conf. on Robotics and Automation*, San Francisco, CA, 2000, pp. 1384–1389.

[7] K. Homma, O. Fukuda, J. Sugawara, Y. Nagata, and M. Usuba, "A wire-driven leg rehabilitatoin system: Development of a 4-DOF experimental system," in *Proc. of IEEE/ASME Int. Conf. on Advanced Intelligent Mechatronics*, 2003, pp. 908–913.

[8] T. Arai, K. Takayama, K. Inoue, Y. Mae, and Y. Kosek, "Parallel mechanisms with adjustable link parameters," in *Proc. of IEEE/RSJ Int. Conf. on Intelligent Robots and Systems*, 2000, pp. 671–676.

[9] L. W. Tsai, "Kinematics of a three-DOF platform with three extensible limbs," in *Recent Advances in Robot Kinematics*, J. Lenarcic and V. Parenti-Castelli, Eds. Kluwer Academic Publishers, 1996, pp. 401–410.

[10] R. Di Gregorio and V. Parenti-Castelli, "A translational 3-DOF parallel manipulator," in *Advances in Robot Kinematics: Analysis and Control*, J. Lenarcic and M. L. Husty, Eds. Kluwer Academic Publishers, 1998, pp. 49–58.

[11] L. W. Tsai and S. Joshi, "Kinematics analysis of 3-DOF position mechanisms for use in hybrid kinematic machines," *ASME J. Mech. Design*, vol. 124, no. 2, pp. 245–253, 2002.

[12] R. E. Stamper, L. W. Tsai, and G. C. Walsh, "Optimization of a three DOF translational platform for well-conditioned workspace," in *Proc. of IEEE Int. Conf. on Robotics and Automation*, Albuquerque, New Mexico, 1997, pp. 3250–3255.

[13] Y. Li and Q. Xu, "Optimal kinematic design for a general 3-PRS spatial parallel manipulator based on dexterity and workspace," in *Proc. of 11th Int. Conf. on Machine Design and Production*, Antalya, Turkey, 2004, pp. 571–584.

[14] C. Gosselin and J. Angeles, "A global performance index for the kinematic optimization of robotic manipulators," *ASME J. Mech. Design*, vol. 113, no. 3, pp. 220–226, 1991.

[15] Y. Li and Q. Xu, "Kinematics and stiffness analysis for a general 3-PRS spatial parallel mechanism," in *Proc. of 15th CISM-IFToMM Symp. on Robot Design, Dynamics and Control*, Montreal, Canada, 2004, Rom04-15.

[16] ——, "Kinematics and inverse dynamics analysis for a general 3-PRS spatial parallel mechanism," *Robotica*, vol. 23, no. 2, pp. 219–229, 2005.

[17] J. J. Craig, *Introduction to Robotics: Mechanics and Control*, 2nd ed. Reading, MA: Addison-Wesley, 1989.

[18] E. G. Gilbert and I. J. Ha, "An approach to nonlinear feedback control with applications to robotics," *IEEE Trans. Syst., Man, Cybern.*, vol. 14, no. 6, pp. 879–884, 1984.